

## Novel composite meshes to evaluate their structural property and *in vivo* biocompatibility for tissue repair

Yao Lu<sup>1</sup>, Shaoju Fu<sup>2</sup>, Bing Hu<sup>1</sup>, Ge Cheng<sup>3</sup>, Nannan Li<sup>1</sup> & Shuanglin Zhou<sup>1,a</sup>

<sup>1</sup> Faculty of Healthcare Equipment, Zhejiang Pharmaceutical College, Ningbo 315000, Zhejiang Province, China

<sup>2</sup> Key Laboratory of Textile Science and Technology, Ministry of Education, Donghua University, Shanghai 201620, China

<sup>3</sup> Medical Engineering Department, The First People's Hospital of Ningbo, Ningbo 315000, Zhejiang Province, China

*Received 1 December 2017; revised received and accepted 27 June 2018*

Composite meshes of different types have been prepared and used for tissue repair in pelvic floor disorder. An interlocking texture mesh (inter-mesh) and a membrane coated mesh (electro-mesh) have been used based on their structural property and biocompatibility. The proportion of degradation material in inter-mesh (69.6%) is found extremely higher than that of electro-mesh (3.22%), thus leading to higher product weight ( $65.50 \pm 2.31 \text{ g/m}^2$ ) and thickness ( $0.500 \pm 0.025 \text{ mm}$ ). After 4 weeks of implantation in animal experiment, inter-mesh with surrounding tissues is observed to have higher breaking strength in tensile behavior and better flexibility. Tissues on inter-mesh are found to grow faster with larger thickness ( $0.76 \pm 0.033 \text{ mm}$ ). The surface area loss of inter-mesh ( $2.49 \pm 0.25\%$ ) is much less than that of electro-mesh ( $7.49 \pm 0.63\%$ ) within the first 2 weeks of implantation. However, the material's degradation is accelerated after 2 weeks, leading to a higher shrinkage of  $13.12 \pm 1.48\%$ .

**Keywords:** Biocompatibility, Electrospinning, Electro-mesh, Interlocking texture, Inter-mesh, Pelvic floor repair, Polypropylene mesh, Polylactic acid mesh

### 1 Introduction

Pelvic floor functional disorder (PFD) is a chronic disease caused by defects, damage or functional disorder of supporting tissues<sup>1</sup>. The status of pelvic floor muscles (PFM) is extremely important, mainly appears as PFM strength, levator hiatus' excessive extensibility, and anterior/central compartment prolapse. Physical training of PFM is a conservative therapy for PFD, which aims to recover and strengthen supportive muscles without surgical injury<sup>2</sup>, but 67% of female patients failed to contract muscles independently in clinical trial, with no curative effect guarantee<sup>3</sup>. Moreover, there are evidences which prove that native tissue-used colporrhaphy cannot effectively correct prolapse, while medical mesh-used treatment is better to support anterior wall<sup>4</sup>.

Polypropylene (PP) mesh with monofilaments interlocking texture is most widely used in tissue repair area. The meshes could be classified based on many elements, including pore size, yarn type, and weight<sup>5,6</sup>. With further research, it was reported that

mesh could also be distinguished by different types of materials. Non-absorbable mesh with permanent material composition, is characterized by stable mechanical property and functions to avoid disease recurrence to a great extent. On the other hand, absorbable mesh with degradation material composition has good biocompatibility, and the burden of this prosthesis on patients could be relieved with the decrease of material amount. To integrate advantages of materials, both non-absorbable and absorbable, the concept of composite mesh has been put forward to widely use in repairing of soft tissues.

Composite mesh is defined as combining absorbable material and non-absorbable material to form an intact structure. Coating an absorbable membrane on non-absorbable macroporous mesh is the most common way to fabricate composite mesh<sup>7,8</sup>. In clinical use, the membrane-coated side is placed against defects to function as anti-adhesion in hernia repair. Another method is to interlace absorbable yarns with non-absorbable yarns by warp knitting technology. Compared to membrane-coated mesh, the interlaced knit mesh still remains macroporous just like traditional PP mesh. Ultrapro<sup>®</sup> (Ethicon, Hamburg, Germany) and Vypro II<sup>®</sup> (Ethicon,

<sup>a</sup>Corresponding author.  
E-mail: zhousl@mail.zjpc.net.cn

Hamburg, Germany) are the two representative products, prepared by PP and polyglactin filaments interlacing<sup>9</sup>. However, Ultrapro<sup>®</sup> is tested to have better clinical effect because of its monofilament yarn type<sup>10</sup>.

Studies<sup>11,12</sup> have shown that composite mesh has less adhesion and inflammation reaction as compared to PP mesh. In our previous study, membrane-coated mesh produced by two coating methods was evaluated, and electrospinning method appeared more superior to solution dipping method.

In this study, an interlocking texture mesh (inter-mesh) and a membrane coated mesh (electro-mesh) have been used for tissue repair in pelvic floor disorder. The meshes are assessed based on their structural property and biocompatibility using animal implantation model.

**2 Materials and Methods**

**2.1 Materials**

Interlocking knit mesh (inter-mesh) and electrospinning membrane-coated mesh (electro-mesh) as prepared in our previous work<sup>13</sup>, were used. The adoption structure and optimal technology parameters were discussed and obtained. Table 1 shows composition, important processing parameters and morphologies of these two composite meshes. Electro-mesh has two-layer structure with a microfibre membrane prepared by electrospinning technology and mesh-like support layer prepared by knitting technology. The microfibre membrane contained polylactic acid (PLA) and poly (ε-caprolactone) (PCL) mixture with weight ratio of 7:3. Raschel knitting machine with gauge of 20E was used for inter-mesh’s fabrication, two bars (GB1,

GB2) drove yarns to move symmetrical, and the formed loops were interlocked to form a hexagon pore-shape mesh.

**2.2 Structural Property**

**2.2.1 Weight**

Samples were balanced under a standard environment (20±2°C, 65±2%) for 24 h before weighing on FA2004A electronic balance. The sample size was 50 mm×50 mm. The final result was expressed by an average value and a standard deviation of 10 repeated tests.

**2.2.2 Absorbable Material Ratio (AM Ratio)**

(i) *Inter-mesh* – The AM ratio of inter-mesh is the percentage of PLA monofilaments weight in the whole composite mesh. It was calculated using the following formula:

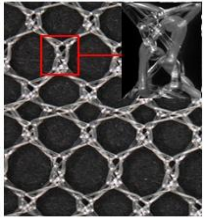
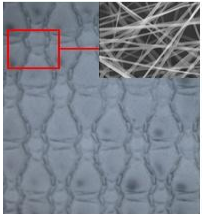
$$AM\ ratio_L = \frac{D_a \times L_a}{D_a \times L_a + D_p \times L_p} \times 100\% \quad \dots (1)$$

where  $D_p$  (tex) is the linear density of PP monofilament;  $L_p$ , the PP monofilaments’ length used in the mesh;  $D_a$  (tex), the linear density of PLA monofilaments; and  $L_a$ , the PLA monofilaments’ length used in the mesh.

Because of the symmetrical motion of two bars in inter-mesh preparation, PP and PLA used were of the same length. The AM ratio is calculated only involving linear density.

(ii) *Electro-mesh* – The AM ratio of electro-mesh is the percentage of PLA/PCL membrane’s weight in the whole composite mesh. It is calculated using the following formula:

Table 1 — Two types of composite mesh

Mesh type	Composition	Fabrication technology	Structure
Inter-mesh	<p><b>PP monofilaments:</b> diameter 0.10 mm, linear density 7.2 tex, stress 58.31 cN/tex.</p> <p><b>PLA monofilaments:</b> diameter 0.15 mm, linear density 7.2 tex, 16.5 tex, stress 30.55 cN/tex.</p>	<p><b>GB1:</b> 21/34/21/23/10/12/10/23// 1 fully 1 empty threaded - PP</p> <p><b>GB2:</b> 23/10/23/21/34/32/34/21// 1 fully 1 empty threaded - PLA</p>	
Electro-mesh	<p><b>PLA/PCL membrane:</b> diameter 412.34±5.8 μm;</p> <p><b>PP mesh-layer:</b> weight 41.19 g/m<sup>2</sup>, thickness 0.412 mm.</p>	<p>Flow rate: 0.6 mL/min; Voltage: 12 KV; Receiving distance: 15 cm</p>	

$$AM_E \text{ ratio} = \frac{W_c - W_p}{W_c} \times 100\% \quad \dots (2)$$

where  $W_c$  ( $\text{g/m}^2$ ) is the weight of composite mesh; and  $W_p$  ( $\text{g/m}^2$ ), the weight of PP mesh used as supporting layer in the membrane-coated composite mesh.

### 2.2.3 Thickness

It was measured according to the standard GB/T3280-1997 using the machine YG141N digital thickness gage. The sample size was 150 mm×150 mm, and area of presser foot was  $2000 \pm 20 \text{ mm}^2$ . The pressure applied on samples was  $1 \pm 0.01 \text{ KPa}$  and lasted for  $30 \pm 5 \text{ s}$ . The final results were expressed by an average value and a standard deviation of 10 repeated tests.

## 2.3 Biocompatibility

### 2.3.1 Surgical Method

Eight wistar female rats weighing 200 - 250 g were randomly divided into two groups. The rats were provided by Tongji hospital, Tongji University, China. The inter-mesh was used in one of the groups and electro-mesh in another group.

Animals were shaved in abdomen area. Anesthetic (1% pentobarbital) was administrated through ear venous. Samples with size of 2 cm×1 cm were implanted through a 2 cm long abdominal incision. Two meshes were implanted in one animal and symmetrically distributed with around an abdominal midline. Meshes were sutured in the center and then closed skins.

During the experiment, all animals were housed under a standard environment (temp. 15 - 25 °C, humidity 60-79%). Water and fodder were provided every day at regular time interval. Two animals in each group were sacrificed by air embolism after 2 weeks and 4 weeks of implantation respectively. The meshes and surrounding tissues were taken out and then fixed in a formalin solution.

### 2.3.2 Biomechanical Property

**Tensile Strength**—Machine YG(B)026G-500 universal testing system was used for tensile behavior measurement. The fixed mesh-tissue complexes were taken out from formalin solution and immediately tested, as these complexes would quickly dry out in air. To avoid slippage, brown paper was used to pack the two ends of samples and then samples were clamped between jaws. The gauge length was 15 mm, extension speed was 50 mm/min, and pre-tension was 1 N. The final result was expressed by an average of repeated tests and a standard deviation.

**Initial Modulus**—The flexibility of samples was presented by initial modulus and calculated from the curve obtained in tensile measurement. It was calculated using the following equation:

$$\text{Initial modulus (MPa)} = \frac{E_{1\%}}{d \times t} \times 100 \quad \dots (3)$$

where  $E_1$  (N) is the load applied on the samples at strain of 1%;  $d$  (mm), the thickness; and  $t$  (mm), the width.

### 2.3.3 Tissue Thickness

Tissue thickness was measured using the machine CH-1-B latex thickness gauge provided by Tianchuang, China. Because of the samples' elasticity, data was read and recorded after 10 s. Five points were randomly selected and tested in each sample. The final average results of the repeated tests were thickness of mesh-tissue complex. The tissue thickness was translated after removing mesh thickness. The final result was expressed by an average value and a standard deviation.

### 2.3.4 Morphological Evaluation of Mesh-tissue

The samples were taken out and dried from formalin solution. They were cut into 1 mm×1 mm square shape with center of a loop and then pasted on stage. The samples were observed under HITACHI S-3003 scanning electron microscope (Hitachi, Japan) after spray-gold finishing.

### 2.3.5 Shrinkage

Shrinkage was considered as area decrease of implanted meshes. Samples were portrayed through a transparent film and pictures were uploaded into computer. The mesh area decrease was calculated from pixel value using Photoshop CS6 software.

## 3 Results and Discussion

### 3.1 Structural Property

Table 2 shows structural property of inter-mesh and electro-mesh. Significant differences are observed between these two types of meshes. The inter-mesh is found toward extremely thicker and heavier, with much more degradable materials. The AM ratio of inter-mesh reaches to 69.6%, indicating that PLA is actually the major component rather than PP. On the other hand, electro-mesh mainly consists of non-

Table 2 — Structural parameters of inter-mesh and electro-mesh

Mesh type	Weight, $\text{g/m}^2$	AM ratio, %	Thickness, mm
Inter-mesh	65.50±2.31	69.6	0.500±0.025
Electro-mesh	42.56±1.28	3.22	0.439±0.018

absorbable PP, with only 3.22% absorbable membrane occupation. The addition of PLA/PCL membrane does not have much effect on mesh thickness and weight.

Compared to the PP-based electro-mesh, inter-mesh shows large increase in thickness and weight. The inherent high stiffness and strength of PLA monofilaments cause this change. For electro-mesh, a membrane covers the entire surface but only occupy 3.22% of weight, related to the electrospinning microfiber's high specific area feather. Based on this, knitting technique by interlacing yarns causes great changes in composite mesh's thickness and weight, while coating method especially by electrospinning technique mainly affects mesh's superficial morphology.

The addition method of absorbable material in composite mesh also decides degradation property. According to theoretical analysis, inter-mesh weight decreases to 19.9 g/m<sup>2</sup> after complete degradation, with large change in mesh structure (looser loop structure, and larger porosity with pore-size). In contrast, the weight loss of electro-mesh will not be high, but completely losing its original smooth membrane.

Composite mesh is expected to fulfill a better biocompatibility as well as post-operative effect<sup>14</sup>. For inter-mesh, the degradable material addition could increase mesh stiffness, help medical staffs to accurately place mesh at the repaired position and avoid crimp. With the degradation of PLA, mesh is also expected to remain softness and lightweight, thus reducing the burden on human body. For electro-mesh, the PLA/PCL membrane avoids severe adhesion. The two types of composite mesh have their own advantage, and hence should be chosen according to the specific condition.

### 3.2 Biocompatibility

#### 3.2.1 Bio-mechanical Property

Figure 1(a) shows breaking strength in mesh-tissue tensile behavior. The breaking strength is increased along with the implantation time. Inter-mesh with surrounding tissues is always stronger than electro-mesh with tissues.

The increase in mesh-tissue's tensile strength is caused by the tissue growth. Considering breaking strength in tensile behavior, tissues are observed to have stable growth tendency. So inter-mesh and electro-mesh are proved to have good biocompatibility for supporting tissue growth.

There are two reasons for the higher breaking strength in inter-mesh. The first is the inherent strength advantage of inter-mesh brought by thicker and stronger PLA monofilaments. While electro-mesh mainly consists of PP monofilaments, the additive membrane layer barely affects mesh strength. Therefore, inter-mesh is inherently stronger than electro-mesh even before implantation (0 week: inter-mesh 16.9±1.3 N, electro-mesh 13.1±0.85 N breaking strength). This strength advantage can stably be retained because of PLA's long degradation period. The second reason for this higher breaking strength is the major ingredient - PLA in mesh, which is beneficial for mesh biocompatibility and also supports more tissue grow.

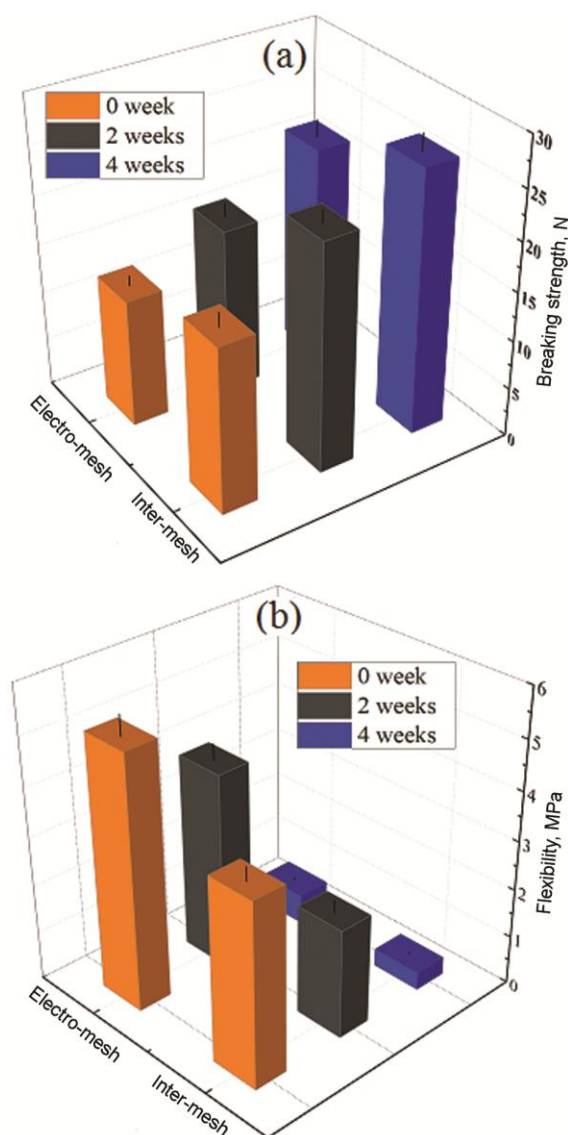


Fig. 1 — Mechanical property of inter-mesh and electro-mesh (a) tensile strength and (b) flexibility

Figure 1(b) shows initial modulus of inter-mesh and electro-mesh, used to characterize mesh flexibility. Low initial modulus corresponds to a good flexibility. The initial modulus of both types of mesh-tissue complexes decrease along with the implantation time, showing that mesh-tissue complexes become more flexible.

Similar to the tensile strength, decrease in initial modulus is also caused by tissue growth. New fresh tissues are much softer than the composite mesh, leading to a continuous increase in the mesh-tissue complex's modulus. The initial modulus of electro-mesh is higher than that of inter-mesh, which proves that electro-mesh is much stiffer. It seems contradictory to the conclusion that thicker and stiffer PLA monofilaments make inter-mesh much stiffer. It is related to the testing method and sample size used in this work. According to our previous study, the PP mesh in electro-mesh had obvious anisotropy, showing that mesh is much stiffer and stronger in longitudinal direction<sup>15</sup>. In the animal experiment, meshes are uniformly cut and implanted along longitudinal direction; bio-mechanical property expressed in this work actually refers to only in longitudinal direction. Even the whole stiffness of inter-mesh is higher than that of electro-mesh, its anisotropy still leads to electro-mesh being stiffer in the longitudinal direction.

### 3.3 Tissue Thickness

Figure 2(a) shows tissue thickness of inter-mesh and electro-mesh, which indirectly expresses tissue growth like tensile strength. The tissue thickness continuously increases both for inter-mesh and electro-mesh (4 weeks: inter-mesh  $0.77\pm 0.053$  mm and electro-mesh  $0.576\pm 0.042$  mm thickness).

After 4 weeks of implantation, the growing tissues are much thicker than the mesh itself, no matter for inter-mesh or electro-mesh. The mesh-tissue complexes mainly consist of tissue layer after then. Inter-mesh is proved to have faster tissue growing speed by the higher tissue thickness. More tissues are able to adhere and grow on the inter-mesh compared with that on electro-mesh. The same conclusion is also proved by the above bio-mechanical property.

### 3.4 Shrinkage

Figure 2(b) shows shrinkage of inter-mesh and electro-mesh after implantation. The shrinkage is increased with the implantation. The longer the implantation, the bigger is the loss in mesh area.

The inter-mesh's shrinkage is only  $2.49\pm 2.5\%$  after 2 weeks of implantation, but it fastly increases to  $13.12\pm 1.48\%$  in the next 2 weeks. The electro-mesh obviously shrinks in the first 2 weeks with mesh area decrease of  $7.49\pm 0.63\%$ , but the overall mesh area loss is smaller, only to  $10.74\pm 0.89\%$ .

Weight and anisotropy are the two main factors affecting mesh shrinkage<sup>16</sup>. It is generally believed that large weight and stiffness are beneficial for stabilizing mesh shape and reducing shrinkage. However, the theory is not comprehensive, and some contradictory results are reported<sup>17</sup>. Currently, the

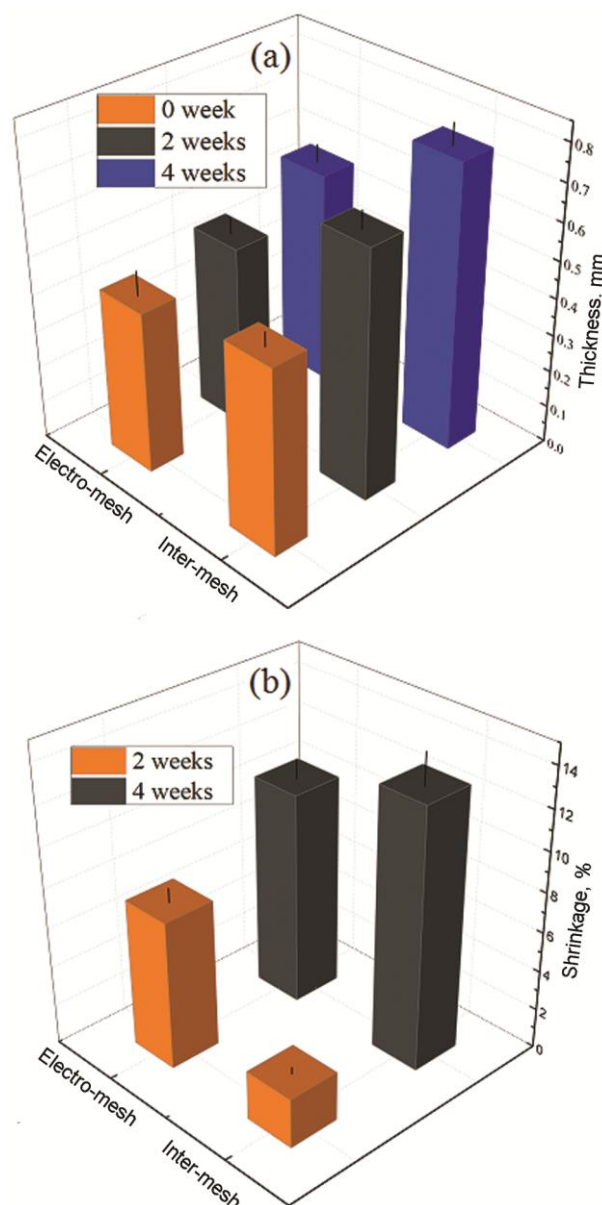


Fig. 2 — (a) Tissue thickness and (b) shrinkage of inter-mesh and electro-mesh

research on mesh structure focuses on the anisotropy<sup>18,19</sup>, and not restricted to weight and thickness. The shrinking phenomenon of medical mesh is also a deformation process by external force, divided into two steps. In the first step, curved yarns are straightened. In the second step, force is applied on the whole mesh and transferred to inner fibres, leading to fibres deformation. The deformation and shrinkage of medical mesh is affected by mesh elasticity, mainly decided by stiffness resistance of fibres. Therefore, mesh tends to shrink along the direction with low stiffness, leading to length decrease in this direction and length increase in the vertical direction.

The PP support in electro-mesh has significant anisotropy with higher longitudinal stiffness. According to the above theory, mesh deformation is an attenuation process. That means, mesh's length would be decreased and loops' distribution would be more concentrated along transverse direction. It leads to the higher shrinkage of electro-mesh in the first 2 weeks. For inter-mesh, the similar stiffness along both the directions stabilizes mesh shape in a short period, and mesh shrink is balanced along both longitudinal and transverse directions. However, the degradable property of PLA materials in inter-mesh causes its large area change in the next 2 weeks. Although a 4 week-period is not long enough for PLA degradation, the slippage of macromolecular chain decreases PLA strength and improves

flexibility. Therefore, inter-mesh shrank obviously during 2 - 4 weeks after implantation, also has a higher final shrinkage than electro-mesh.

**3.5 Morphological Evaluation of Mesh-tissue**

Figure 3 shows morphological structures of inter-mesh and electro-mesh with the surrounding tissues. After 2 weeks of implantation, mesh's loop structures are clearly observed for both meshes under a low magnification. The tissue layers are covered with meshes having loosen structures and low thickness. Then magnification is enlarged to analyze tissue micro-structure, clear fibrosis structures are found on the both mesh surfaces, with obvious texture feature. No significant difference of morphologies is found between electro-mesh and inter-mesh.

However, obvious changes are observed within different implantation time. After 4 weeks, the former clear loop structures are disappeared under the thicker tissue layer. Moreover, the fibrosis structure is also replaced by a relative smooth structure.

The morphologies of inter-mesh and electro-mesh show much more mature tissues after 4 weeks, with significant increase in thickness. During the initial stage of implantation, fresh tissues cannot completely adopt to the prosthesis and tend to grow away from it, leading to an intensive tissue distribution and texture surface formation. After 4 weeks of implantation, tissues adapted to the existence of medical mesh, grow along and also become tightly close to the mesh shape, forming a relative smooth surface.

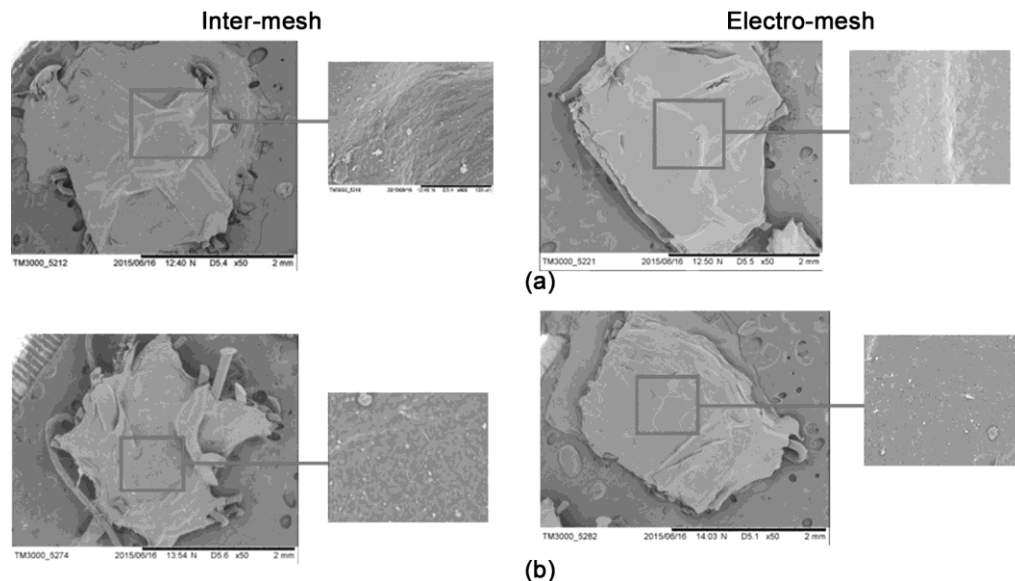


Fig. 3 — Morphologies of inter-mesh and electro-mesh with the surrounding tissues (a) two weeks after implantation and (b) four weeks after implantation

#### 4 Conclusion

The medical mesh studied in this work is used for supporting prolapsed organs or repairing damaged tissues in pelvic floor area. Two different types of composite meshes are compared based on their structural parameters and *in vivo* biocompatibility.

Inter-mesh is found significantly different from electro-mesh from the outside even if both are composed of PP and PLA materials. The inter-mesh formed by interlacing PLA monofilaments with PP filaments is manufactured using warp knitting technology, with mesh-structure appearance just like traditional single component PP mesh, but with increased thickness and weight property. The electro-mesh coated by a thin and light microfiber membrane show obvious changes in superficial morphology, but its structural parameters are barely affected.

After measuring mesh structural property, the *in vivo* biocompatibility is evaluated by implantation in animals. Overall, both inter-mesh and electro-mesh show good biocompatibility, and can support tissue growth in the 4-weeks implantation. However, tissues on the inter-mesh has faster growing speed because of the high PLA content. Inter-mesh with the surrounding tissues is much stronger and more flexible than electro-mesh, can support prolapsed organs and reduce patient discomfort more effectively. PLA monofilaments' degradation shows larger shrink in mesh during the last stage of implantation ( $13.12 \pm 1.48\%$ ), resulting in a unstable shape and size in sample appearance. For both meshes, the overlapped tissues are proved to be normal, with a process evidence that the tissue becomes more mature at the last stage.

Warp knitting technology and coating methods are proved to be useful for composite mesh preparation. However, they both have some flaws in property.

#### Acknowledgement

Authors are thankful for the funding support by education department of Zhejiang Province of China (Project reference number Y201942805).

#### References

- 1 Pushkar D Y, Vasilchenko M I & Kasyan GR, *Int Urogynecology J*, 10 (24) (2013) 1765.
- 2 Özdemir Ö Ç, Bakar Y, Özengin N & Bülent D, *J Phys Therapy Sci*, 27 (7) (2015) 2133.
- 3 Kim S, Wong V & Moore K H, *Australian, New Zealand J Obstetrics Gynaecology*, 53 (6) (2013) 574.
- 4 Altman D, Vayrynen T, Engh M E & Susanne M A, *New England J Medicine*, 53 (1) (2011) 1826.
- 5 Krause H, Bennett M, Forwood M & Judith G, *Int Urogynecology J*, 19 (2008) 1677.
- 6 Feola A, Abramowitch S, Jallah Z & Suzan S, *Bjog-Int J Obstetrics Gynaecology*, 120 (2) (2013) 224.
- 7 Fujino K, Kinoshita M, Saitoh A, Yano H, Nishikawa K, Fujie T, Iwaya K, Kakihara M, Takeoka S, Saitoh D & Tanaka Y, *Surg Endosc*, 25 (10) (2011) 3428.
- 8 Zhang Z, Zhang T, Li J, Ji Z L, Zhou H, Zhou X F & Gu N, *J Biomedical Mater Res [Part B], Appl Biomater*, 102 (1) (2013) 12.
- 9 Schug-Paß C, Tamme C, Sommerer F, Tannapfel A, Lippert H & Köckerling F, *Surgical Endoscopy*, 22 (4) (2008) 100.
- 10 Smietański M, Bigda J, Zaborowski K, Worek M & Śledziński Z, *Hernia*, 13 (3) (2009) 239.
- 11 Liang R, Zong W, Palcsey S, Abramowitch S & Moalli P A, *Am J Obstetrics Gynaecology*, 212 (2) (2015) 174.
- 12 Huber A, Boruch A, Medberry C, Honerlaw M & Badylak S F, *J Biomed Mater Res [B]*, 100B (1) (2012) 145.
- 13 Lu Y, Chen Y C & Zhang P H, *Fibers Text East Eur*, 24 (3) (2016) 17.
- 14 Cobb W S, Kercher K W & Heniford B T, *Surgical Innovation*, 12 (1) (2015) 63.
- 15 Lu Y & Zhang PH, *Text Res J*, 87 (12) (2016) 1275.
- 16 Jerabek J, Novotny T, Vesely K, Cagas J, Jedlicka V, Vlcek P & Capov I, *Hernia*, 18 (2014) 855.
- 17 Yuri W N, Andrew G H, Joseph A C, Paton B L, Norton H J, Peindl R D, Kercher K W & Heniford B T, *J Surgical Res*, 140 (2007) 6.
- 18 Anurov M V, Titkova S M & Oettinger A P, *Hernia: J Hernias Abdominal Wall Surgery*, 16 (2) (2011) 199.
- 19 Alizai P H, Schmid S, Otto J, Klink C D, Roeth A, Nolting J, Neumann U P & Klinge U, *J Biomedical Mater Res [Part B], Appl Biomaterials*. 102 (7) (2014) 1485.